
Positive-Negative Equal Contrastive Loss for Semantic Segmentation

Jing Wang^{1*} Lingfei Xuan^{1*} Wenxuan Wang¹ Tianxiang Zhang¹ Jiangyun Li^{1†}
¹University of Science and Technology Beijing

Abstract

The contextual information is critical for various computer vision tasks, previous works commonly design plug-and-play modules and structural losses to effectively extract and aggregate the global context. These methods utilize fine-label to optimize the model but ignore that fine-trained features are also precious training resources, which can introduce preferable distribution to hard pixels (i.e., misclassified pixels). Inspired by contrastive learning in unsupervised paradigm, we apply the contrastive loss in a supervised manner and re-design the loss function to cast off the stereotype of unsupervised learning (e.g., imbalance of positives and negatives, confusion of anchors computing). To this end, we propose **Positive-Negative Equal** contrastive loss (PNE loss), which increases the latent impact of positive embedding on the anchor and treats the positive as well as negative sample pairs equally. The PNE loss can be directly plugged right into existing semantic segmentation frameworks and leads to excellent performance with neglectable extra computational costs. We utilize a number of classic segmentation methods (e.g., DeepLabV3, HRNetV2, OCRNet, UperNet) and backbone (e.g., ResNet, HRNet, Swin Transformer) to conduct comprehensive experiments and achieve state-of-the-art performance on three benchmark datasets (e.g., Cityscapes, COCO-Stuff and ADE20K). Our code will be publicly available soon.

1 Introduction

Semantic segmentation, which aims to classify each pixel in the visual area, is employed in many practical scenes (e.g., autonomous driving and clinical assistance). As an essential task in exploring semantic representation for scene understanding, semantic segmentation is driven by pixel-level labeled data and ingenious segmentation networks.

For dense prediction tasks like semantic segmentation, both local and global context are critical. Based on Fully Convolutional Network (FCN) [1], several works explore module-based methods to exploit or aggregate contextual information from the visual representation of pixel embeddings, e.g., pixel-to-pixel attention mechanism [2, 3], multi-layer dilated convolution [4, 5] and pyramid pooling operation [6]. However, these proposed frameworks include two-fold shortcomings. Firstly, the process of extracting informative context in [2, 3, 4, 5, 6] is a passive pattern without any supervision. Secondly, complex relationships between large amount of pixels in an image lead to unbearable computational overheads. Thus, these methods [2, 3] can not achieve the trade-off between speed and accuracy. Furthermore, these networks commonly use the pixel-wise cross entropy loss function and lack supervised attention on contextual information that contains abundant representation of explicit relationship between pixels.

*Equal Contribution.

†Corresponding Author.

Some other works explore loss-based methods [7, 8] which apply the loss function to guide the network to model relationship between pixels precisely. These research have suggested that constructing intra- and inter-class structured losses can strengthen pixel-to-pixel interactions. To illustrate the importance of this inspiration, we visualize the pixel embeddings of penultimate layer output. As shown in Fig.1, the embedding of correctly classified pixels are more aggregated in embedding space. However, the embedding of wrongly classified pixels, which are generally difficult pixels with semantic confusion, is not uniformly distributed in the expected segmentation embedding space. To solve this problem, a intuitive belief is that more consistent the distribution of difficult pixels and correctly classified pixels is, the higher the probability of hard pixels is correctly classified. Therefore, designing the loss function to optimize the distribution of pixel embedding makes these confused features close to the embedding of precisely classified pixels, which may be a novel way to assist the network to capture contextual information.

Recently, success in self-supervised learning [9, 10] reveal that contrastive learning shows powerful potential by pre-training model without any labeled data. Contrastive learning force model to extract close feature representations from similar samples (positive pairs) and distant feature embeddings from disparate samples (negative pairs). Each image can be reckoned as an anchor, and the positive pair is achieved through the introduced data-augmentation on the current image. At the same time, the negative pair is also constructed from the acquired different image samples. This unsupervised paradigm makes pre-training model show outstanding performance on some specific downstream tasks like image classification and object detection. Although this aforementioned unsupervised paradigm achieves promising results, it is difficult to construct appropriate positive samples among the large amount of unlabeled data. Therefore, unsupervised contrastive learning takes advantage of plenty of negative samples which are selected from the acquired datasets. In contrast, supervised semantic segmentation with detailed labeled data can better be incorporated with contrastive learning. Last year, [11] extend computational domain from intra-image to inter-image, aiming to gain more global context from positive and negative samples in a training batch. Trying to model explicit semantic relationship of the whole image, [12] save class embedding of every image as comparative samples with the proposed memory bank. With the potential of contrastive learning, they all achieve state-of-the-art performance on semantic segmentation task.

However, such a training paradigm does not effectively integrate the supervised information, which remains two potential drawbacks. **First**, limited by the stereotype from unsupervised learning, the design of contrastive loss is hardly influenced by positive samples. Previous studies [13] have demonstrated that negative pairs instead of positive ones contribute the dominant gradient during back-propagation. So that the attractive force of the anchor to the positive sample is not strong enough. **Second**, while applying contrastive loss to semantic segmentation task, the number of pixel-level samples rapidly increases compared to the image-level samples in classification. But gradients are not calculated separately for anchors which obtain different predictions with the same label. With different distributions in embedding space, anchors will adopt the same direction for optimization.

With above concerns, we propose a novel contrastive loss, named Positive-Negative Equal loss, to supervise pixel-wise embedding by prior knowledge from fine labels. As the common setting, any pixel-wise embeddings extracted by network can be reckoned as a sample. Specifically, positive pairs are constituted with any embedding which correspond to the same category, while the negative pairs are constituted in different category. There are totally two improvements about our proposed loss function. **First**, different from previous work, we modify the calculation method of the loss function

to more focus on the guidance from positive samples. It is easy to acquire plenty of positive pairs with finer embedding from pixels in the same class. These positives are the best learning templates for anchors with confused feature. As for all the sample pairs, positive and negative have equal importance in loss function. An anchor point will calculate cosine distance with positive samples repeatedly in a single operation which is just the same as negative pairs, thereby moving towards more general embedding space. **Second**, we propose a more reasonable pairing method of positive and negative sample pairs, which reduces the amount of computations and makes the optimization direction of the anchor clearer. Only samples which are classified falsely will participate in the calculation as anchor. Furthermore, we prove that contrastive loss is more suitable for the extraction of contextual information in high level embedding space.

The main contributions of this paper are as follows:

- We propose a novel pixel-wise contrastive loss in a supervised manner which pays more attention to positive pairs that are ignored in previous works. It changes contrastive learning paradigm from learning target feature to learning inter class feature embedding space.
- We design an effective sampling strategy to cast off confusion of anchors and negatives. Through the decoupling of negative pairs, PNE loss can calculate the semantic association of negative sample pairs more efficiently and reduce the influence of the weak association samples on anchor.
- We verify the effectiveness of the proposed PNE loss by conducting extensive experiments with several semantic segmentation networks such as, DeepLabV3, OCRNet, on various public datasets (i.e., Cityscapes and COCO Stuff).

2 Related Works

2.1 Semantic Segmentation

FCN[1] uses the fully convolutional network without the full connection layer to achieve the pixel-level prediction task. However, it can only perceive the limited visual context with the local receptive fields, and poorly extract the strong inter-relationship among pixels in an image. Therefore, A lot of research has attempted to enlarge the local sensing domain and enhance the fusion of contextual information for preferably extracting the inter-relationship among pixels. For instance, DeepLab Series[4, 14] employ atrous convolution to increase the receptive fields while ensuring the resolution of the feature map. PSPNet [15] applies multi-scale pooling of the feature pyramids to fuse multi-scale features. U-Net[16] and SegNet [17] adopt the Encoder-Decoder architecture to merge features from different network layers and recover losed information from downsampling. DANet[2] and OCNet[18] employ self-attention mechanism to capture long-range context and directly exchange the contextual information between paired pixels. OCRNet [19] proposes object-contextual representations that characterize a pixel by exploiting the representation of the corresponding object class. In SETR[20] and Segmenter[21], Vision Transformer [22] substitutes traditional convolutional backbones to promote context learning on lower-level feature by self-attention mechanism.

It is clear that these works focus on module design which is poorly initiative in exploring pixel relation. We propose PNE loss to establish the inherent connection between difficult pixels and other strongly correlated pixels, and provide appropriate optimization direction for difficult pixels.

2.2 Contrastive Learning

In self-supervised learning, contrastive learning [23, 24] methods achieve the state-of-the-art result, becoming a major branch in computer vision pretext tasks. It is a discriminative learning manner that contrasts positive (similar) pairs against negative (dissimilar) pairs to learning representations. A vast range of methods based on contrastive manner have been recently proposed. SimCLR [9, 25] proposes a simple framework, where constructs the augmented views of the image as positive pairs and the rest of image in training batch as negative pairs, using huge training batch to exploit many negative pairs efficiently and improve performance. [24, 26] use memory bank to store features of every instance in the dataset, and partly solve the inverse optimization due to large batch. MoCo[10, 27] design a momentum encoder to dynamically update negative pairs and maintain consistent representations of negative pairs per iteration. To improve the optimization efficiency, some works[28, 29, 30]

sample negative pairs according to their cosine similarity. Moreover, [13] probe into the function of temperature hyper-parameter and find it domain the attention of negative pairs in the loss function.

Previous years, some works [11, 12, 31, 32, 33], have adopted pixel-to-pixel contrastive loss and achieve assuring results. They all prove that contrastive learning can bring more structural embedding space for pixels in different classes. But they also can be improved in several points. First, pixel-wise positive samples are easier to get compared to image-wise and can be fully utilized by proper loss function design. Second, anchor points are not grouped clearly. It is distinct that hard pixels have dissimilar distribution in embedding space with different score map and ground-truth. The hard anchor should be regrouped.

2.3 Distribution Optimization

Strong relationship between pixels is important property in image processing. Traditional pixel-wise cross entropy loss formulates it as an independent pixel labeling problem and ignores structure information between pixels. As shown in Fig.1, the clearer distribution of features is, the higher accuracy of the model is. For the optimization of feature distribution, it can be roughly divided into two directions: one is to find a more accurate measurement method. Several ways to exploit the distribution information between pixels have been investigated [7, 8, 34]. RMI[8] models spatial structure in the 3x3 window and emphasizes adjacent neighborhoods. AAF [7] makes a breakthrough at distance computation between pixels than RMI. MCIBI[34] gathers pixel level feature distribution by class level memory bank which is updated during training step. Another one is looking for more suitable teachers. A simple way is label smoothing [35] which improves the distribution of labels by regularization, and it reduces the difficulty of learning targets for model to prevent over-fitting. Furthermore, in some lightweight works, knowledge distillation[36] can bring well distribution of large model to lightweight model.

Combining the above two points, our work provides another perspective on distribution optimizing by deploying contrastive learning in supervised semantic segmentation. The method utilizes high-quality embedding of correctly classified pixels to optimize distribution of major pixels being classified falsely from proper class distribution. Furthermore, distribution optimizing is only used in the segmentation model during training step, without extra inference step during testing.

3 Method

3.1 Contrastive Learning

Supervised pixel-wise contrastive Learning. As common settings, an image $I \in \mathbb{R}^{3 \times H \times W}$ is fed into an encoder-decoder architecture which exports feature maps $F \in \mathbb{R}^{C \times \frac{H}{4} \times \frac{W}{4}}$. Then, the feature maps will go through segmentation head and up-samplings to produce score map $S \in \mathbb{R}^{1 \times H \times W}$ of the prediction. Last year, several works convert contrastive loss from image-size to pixel-size [11, 12], and optimize the contrastive pairs sampling strategy. Positive pairs containing anchor $i \in \mathbb{R}^D$ and positives i^+ are the same class in ground-truth map $G \in \mathbb{R}^{1 \times H \times W}$, but negatives i^- are sampled from different classes in identical image or others. Generally, the conventional loss is defined as:

$$L_i^{NCE} = \frac{1}{|P_i|} \sum_{i^+ \in P_i} -\log \frac{\exp(i \cdot i^+ / \tau)}{\exp(i \cdot i^+ / \tau) + \sum_{N_i} \exp(i \cdot i^- / \tau)}, \quad (1)$$

where for pixel embedding i , P_i denotes the positive embedding set, N_i denotes the negative embedding set and $|P_i|$ denotes numbers of positive pairs. ‘ \cdot ’ means the inner (dot) product.

Project Head. SimCLR [9] adds MLP as the project head in contrastive learning for the first time. In subsequent works, MLP has been widely used because of its superiority. [37] does extensive research on MLP and verifies the effect of MLP on the embedding space on computer vision task.

Loss Combining. As stated in Eq. 1, L^{NCE} is designed to adjust the embedding space, and not to force the network to output symbolic results. Fortunately, the cross entropy loss used widely in semantic segmentation task can represent the difference between the sample label and the predicted probability. Following [11], the function can be formed as:

$$L_i^{CE} = -1_c^\top \log(\text{softmax}(y)), \quad (2)$$

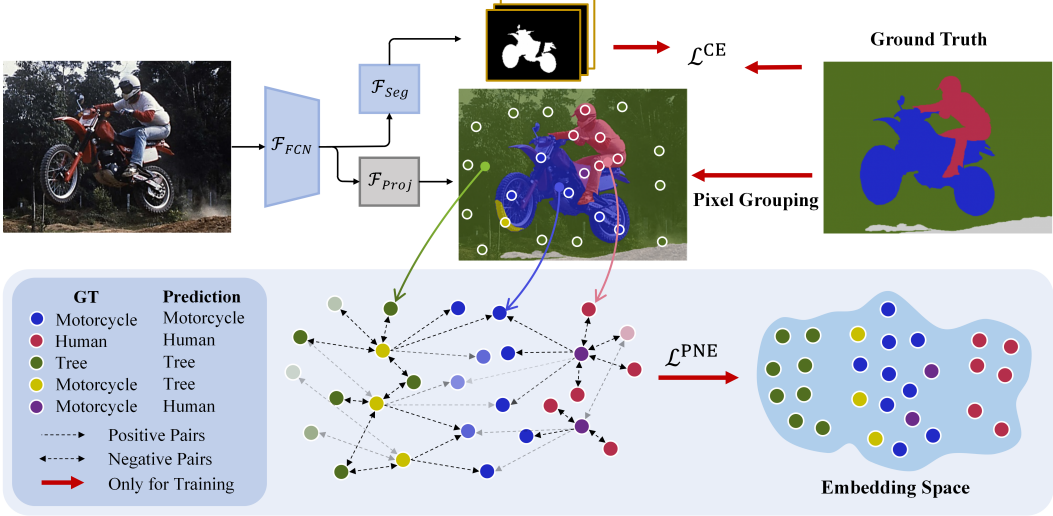


Figure 2: The overall architecture and design details of the proposed PNE loss. Pixel embedding extracted by \mathcal{F}_{proj} and \mathcal{F}_{FCN} . For per class, pixel embeddings are grouped into correctly classified and each misclassified category according to Ground Truth (GT) and predictions from \mathcal{F}_{seg} . The property of the misclassified pixel embeddings point out the classes of positive and negative samples. The anchors, positives and negatives are all randomly sampled from limited regions respectively.

where $1_{\bar{c}}$ denotes the one-hot encoding of \bar{c} , the logarithm is defined as element-wise, and $\text{softmax}(y_c) = \exp(y_c) / \sum_{c'=1}^{|C|} \exp(y_{c'})$.

The supervisory information (from $G \in \mathbb{R}^{1 \times H \times W}$) utilized by cross entropy loss is poor but distinct. Meanwhile, the information (from $F \in \mathbb{R}^{C \times \frac{H}{4} \times \frac{W}{4}}$) utilized by L^{NCE} is obscure but abundant. It is obvious that their information types are complementary. As shown in Fig.2, cross entropy loss can provide simple but clear pixel categories, and L^{NCE} can optimize the feature representation of anchor in high-dimension space and adjust the structural similarity between pixel embeddings. The combined function used for training the model is:

$$L_i^{COM} = L_i^{CE} + \alpha L_i^{NCE}, \quad (3)$$

where the L_i^{COM} can directly act on segment head, and α is weight factor.

3.2 Balance of Positives and Negatives

More attention to positives. As stated in 2.3 and 3.1, supervised contrastive learning is limited by unsupervised paradigm which struggles in lack of positive samples. However, with the help of labeled data, positive pairs sampled from same class are not scarce anymore. [13] proves that optimized gradient of L_i^{NCE} like Eq.1 and Eq.2 is mostly from negative pairs. That situation will make model prefer to separate anchor from negatives rather than gather anchor and positives. Let us consider a normal situation for Eq.1: to simplify, we refer a_p, b_n to $\exp(i \cdot i^+ / \tau), \exp(i \cdot i^- / \tau)$:

$$\begin{aligned} L_i^{NCE} &= \frac{1}{|P_i|} \sum_{p \in P_i} -\log \frac{a_p}{a_p + \sum_{n \in N_i} b_n} \\ &= [\sum_{p \in P_i} \log(1 + \sum_{n \in N_i} b_n / a_p)] / P \\ &\approx \log(1 + (\sum_{n \in N_i} b_n) / \bar{a}) \\ &= \log(1 + N\bar{b} / \bar{a}), \end{aligned} \quad (4)$$

where P and N are numbers of positive and negative pairs, \bar{a} and \bar{b} are average of a_p, b_n . It is obvious that negative pairs provide most of penalty value. At final stage of the training, a_p will approximate

to b_n , and the Eq.4 can be simplified to $\log(1 + N)$. The value of PNE loss will be decided by numbers of negatives pairs.

As shown in Fig.1, the distance between classification centers and the separability of category boundaries are both important for classification task. Therefore, we need to improve the form of L^{NCE} to cluster the embedding of every category. With this insight, we put more weight to positive pairs in logarithm function by transferring summation of positives. After simplified, our loss function is defined as:

$$L_i^{NCE} = \log\left(1 + \frac{\sum_{i^- \in N_i} \exp(i \cdot i^- / \tau)}{\sum_{i^+ \in P_i} \exp(i \cdot i^+ / \tau)}\right). \quad (5)$$

As Eq.4 setting, the Eq.5 can be simplified to:

$$\begin{aligned} L_i^{NCE} &= \log\left(1 + \frac{\sum_{n \in N_i} b_n}{\sum_{p \in P_i} a_p}\right) \\ &= \log\left(1 + N\bar{b}/P\bar{a}\right) \\ &= \log\left(1 + \bar{b}/\bar{a}\right), \quad \text{if } N = P \end{aligned} \quad (6)$$

In this work, we set $N = P$ to treat negative and positive pairs equally. We can see that the improved PNE loss ignores the influence of pairs number and is only calculated by cosine distance of pairs.

Per-positive Weight. Following the Eq.5, we construct a region-to-pixel contrastive learning strategy with positive and negative pairs. In this way, all samples can be utilized for the optimization of network. However, there is different importance in each sample.

For positives, we introduce prediction score to adjust the weights of each positive sample. As a whole, their value is undoubtedly, but the quality of the individual samples are various. If the final score of a pixel is higher, the pixel embedding after the segmentation head is more separable. With this idea, we use the cosine distance of positive pair (i, i^+) to multiply with prediction score s_{i^+} after *softmax*, which means that high-quality positive features will be paid more attention. The mathematical expression can be defined as:

$$L_i^{NCE} = \log\left(1 + \frac{\sum_{i^- \in N_i} \exp(i \cdot i^- / \tau)}{\sum_{i^+ \in P_i} w_{i^+} / \bar{w}_+ \cdot \exp(i \cdot i^+ / \tau)}\right), \quad (7)$$

where \bar{w}_+ represent the average of w_{i^+} .

But for negatives, refinement of every negative pair is not necessary. Individually, the cosine similarities of negative pairs have already decided gradient contribution from every negative sample to specific anchor. The feature quality of single negative sample has no obvious significance of reference for anchor from other categories. As a whole, anchors need to be far away from all of them in embedding space. The weights change of single pairs do not contribute much to the entirety of negative samples. We provide the corresponding experiments of the positive weighting in ablation study.

3.3 Construction Strategies

Individual anchor sets. Directly converting contrastive learning from image-wise to pixel-wise faces computation limits without sampling. Previous works provide several feasible ways which focus on improving the discrimination power of models by sampling hard anchors (the pixel with incorrect predictions). However, these strategies still exist embedding confusion and computational waste in negative pairs. As shown in Fig.2, hard anchors, containing different individual set $S_{l,k}$ (l means predicted result, k means ground-truth label), are classified as different classes $\tilde{\mathbb{C}}$ ($l \in \tilde{\mathbb{C}}$, and $\tilde{\mathbb{C}} \subset \mathbb{C} \setminus k$, where $\mathbb{C} \setminus k$ denotes the pixels belonging to the classes except class k). They are distributed in different embeddings space, even though have same class k in ground-truth. It is unreasonable that the hard anchors in different distribution are guided by same negative samples. In our method, hard anchors with same ground-truth label but different predicted results are divided into individual sets which will be calculated separately, not mixed up anymore.

Corresponding negatives. In semantic contrastive learning[13, 30], negative samples should select pixels similar to the anchor as much as possible. During calculating contrastive loss, utilizing

difficult-to-distinguish negative samples can optimize pixel embedding space faster. In this paper, we use semantically explicit category information to select difficult negative samples instead of cosine similarity used in previous works [13, 30]. Cosine distance can not accurately measure embedding similarity which usually refers to surrounding structural information and modulo of a vector in addition. Instead of using cosine similarity, it is better to select difficult negative samples by obvious classificatory information from label. In details, for samples with the same predictions, their similarity is naturally closer than others. The individual anchor set $S_{l,k}$ are more similar to $i_{l,l}$ (pixel set that left l means predicted result and right l means label) which have same predicted result. Thence, corresponding negatives $N_{l,l}$ for individual anchor set $S_{l,k}$ are only sampled from $i_{l,l}$ in PNE loss.

In this way, the negative pairs, constructed by these individual anchor sets and corresponding negatives, will be calculated more simply without filtering anchor and negatives by their difficulty. Furthermore, the anchors will be optimized more pertinently by their corresponding negatives. Meanwhile, all of anchors will not lose context information contrast to other contrastive loss because all relevant negatives were calculated with a pair scale. Thus, the supervised contrastive loss is defined as:

$$L^{PNE} = \frac{1}{|S|} \sum_{l \in C} \sum_{k \in C \setminus l} \sum_{i \in S_{l,k}} \log \left(1 + \frac{\sum_{i^- \in N_{l,l}} \exp(i \cdot i^- / \tau)}{\sum_{i^+ \in P_{k,k}} w_{i^+} / \bar{w}_+ \cdot \exp(i \cdot i^+ / \tau)} \right), \quad (8)$$

where $|S|$ denotes the numbers of pixels with incorrect predictions. Similar as $N_{l,l}$, $P_{k,k}$ are sampled from $i_{k,k}$. $|S| < 200$ is set to save computation resources.

4 Experiment

In this section, we conduct comprehensive experiments to evaluate the PNE loss on three popular segmentation datasets, including Cityscapes, COCO-Stuff and ADE20K.

4.1 Datasets and Evaluation Metrics

Datasets. Our experiments are conducted on two datasets: **Cityscapes** is a large-scale dataset for segmentation task, which is collected from 50 different urban street scenes. The dataset contains 5K finely annotated images and 20K coarsely annotated images of driving scenes. The 5K finely annotated images used in our experiment are divided into 2,975, 500, 1,525 images for training, validation and testing respectively. **ADE20K** is a widely-used semantic segmentation dataset, containing up to 25K images in 150 categories that are densely annotated. The 25K images are split into sets with numbers 20K, 2K, 3K for training, validation and testing. **COCO-Stuff** is a large-scale benchmark which is applied for instance segmentation as well as semantic segmentation, providing rich annotations for 91 thing classes and 91 stuff classes. The dataset has 10K images, which is partitioned into 9K images for training and 1K images for validation.

Evaluation metric. The standard mean Intersection of Union (mIoU) is chosen as the evaluation metric. Following general protocol[11, 12], we average the segmentation results over multiple scales with flipping, i.e., the scaling factor is 0.75 to 2.0 (with intervals of 0.25) times of the original image size. For ablation studies, the single-scale evaluation is performed if not mentioned.

4.2 Implementation Details

We select DeepLabV3, OCRNet, HRNetV2 and UperNet as our baseline, and apply HRNetV2, ResNet-101 and Swin-B as backbone pretrained on ImageNet. PNE loss is developed on mmsegmentation toolbox [38], and attached to DeepLabV3, OCRNet and Swin-Transfomer to validate the generalization ability. Additionally, we plug the PNE loss into the position behind bottleneck as stated in Sec. 3.3 and implement our method based on Pytorch [39]. Following [11, 12], our model is trained with Stochastic Gradient Descent (SGD). During the training phase, a poly learning rate policy is employed where the initial learning rate is multiplied by $(1\text{-iter/total_iter})^{0.9}$ after each iteration. The base learning rate is set to 0.001 for COCO-Stuff and 0.01 for Cityscapes and ADE20K. Momentum and weight decay coefficients are set to 0.9 and 0.0001 respectively. The batch size is set to 8 for Cityscapes and 16 for COCO-Stuff and ADE20K. Meanwhile, the training time is set to 40K steps for Cityscapes and 60K steps for COCO-Stuff. In addition, random scaling, random cropping, and random left-right flipping are applied as data augmentation during training.

4.3 Comparison to State-of-the-Arts

Cityscapes. We present the evaluation results of the proposed method on Cityscapes validation and test set and compare them with other state-of-the-art methods in Table 1. We find that, with a small increase in training time, the accuracy of model on the validation and test set can be improved considerably without sacrificing inference time. Specifically, the performance of DeepLabV3 improved **2.3%** mIoU on validation set from 78.5% to 80.8% and **1.2%** mIoU on test set from 78.1% to 79.3% by PNE loss. Simultaneously, OCRNet with our method yields the mIoU of 82.9% and 81.7% on validation and test set respectively. Both of the improvements demonstrate the proposed PNE loss can effectively promote the performance of baseline as expected. To be mentioned, the settings of all the above testing results are based on multi-scale and flipping tricks.

Table 1: Results on the Cityscapes val and test set.

Method	Backbone	sec./iter.	val mIoU%	test mIoU%
AAF[7]	D-ResNet-101	-	79.2	79.1
DeepLabV3+[40]	D-Xception-71	-	79.6	-
PSPNet[41]	D-ResNet-101	-	79.7	78.4
DANet[2]	D-ResNet-101	-	81.5	-
HANet[42]	D-ResNet-101	-	80.3	-
SpyGR[43]	D-ResNet-101	-	80.5	-
ACF[44]	D-ResNet-101	-	81.5	-
EncNet [†] [45]	D-ResNet-101	-	77.1	-
EncNet + Ours	D-ResNet-101	-	77.7(+0.6)	-
DeepLabV3[14]	D-ResNet-101	1.92	78.5	78.1
DeepLabV3 + CIPC[11]	D-ResNet-101	-	-	79.2(+1.1)
DeepLabV3 + Ours	D-ResNet-101	2.43	80.8(+2.3)	79.3(+1.2)
HRNetV2[19]	HRNetV2-W48	0.57	79.7	79.4
HRNetV2 + CIPC[11]	HRNetV2-W48	-	81.0(+1.3)	81.4(+2.0)
HRNetV2 + Ours	HRNetV2-W48	0.64	81.5(+1.8)	80.6(+1.2)
OCRNet[19]	HRNetV2-W48	1.40	81.6	80.4
OCRNet + Ours	HRNetV2-W48	1.65	82.9(+1.3)	81.7(+1.3)

Table 2: Results on the COCO-Stuff test set.

Method	Backbone	mIoU%
SVCNet[46]	D-ResNet-101	39.6
DANet[2]	D-ResNet-101	39.7
SpyGR[43]	ResNet-101	39.9
ACNet[47]	ResNet-101	40.1
DeepLabV3 [†] [14]	D-ResNet-101	38.8
DeepLabV3 + Ours	D-ResNet-101	39.2(+0.4)
UperNet[48]	Swin-B[49]	43.7
UperNet + Ours	Swin-B	44.3(+0.6)

Table 3: Results on the ADE20K val set.

Method	Backbone	mIoU%
CFNet[50]	D-ResNet-101	44.89
CCNet[51]	D-ResNet-101	45.22
GANet[52]	D-ResNet-101	45.36
OCRNet[19]	HRNetV2-W48	45.66
OCRNet + Ours	HRNetV2-W48	46.76(+1.10)

COCO-Stuff. Table 2 presents excellent results produced by PNE loss on COCO-Stuff test set. [†] denotes results posted by mmsegmentation toolbox. Our method outperforms DeeplabV3 by **0.3%** mIoU and Swin-B by **0.6%** mIoU. The great improvements illustrate that PNE loss can guide the baseline more effectively capture complicated contextual representation. Besides, the visual comparison also proves the improvement with PNE loss. As shown in Fig.3, our method achieves more precise prediction than baseline (like the region of dog in right second row).

ADE20K. Models trained with PNE loss show better capturing ability of context in scene parsing compared to those without PNE loss. As shown in Table 3, the improvements of our method are **1.10%** mIoU in OCRNet.

4.4 Ablation Study

In this subsection, extensive ablation studies are performed on the Cityscapes validation set to verify the effectiveness of our ideas. Unless explicitly specified otherwise, all experiments are conducted on the DeepLabV3 with Dilated-ResNet-50 backbone. We choose DeepLabV3-R50 with cross entropy loss function as our baseline.

Equal calculation. We carry out experiments to evaluate the effectiveness of the proposed positive-negative equal contrast. As shown in Table 4, the model with PNE contrastive loss brings the improvement of **3.9%** mIoU than baseline. Compared with traditional contrastive loss, PNE contrastive loss also helps obtain significant improvement at least **1.5%** mIoU. This illustrates positive-negative equal contrast is more suitable than normal contrastive loss, which is widely applied on unsupervised way in semantic segmentation.

Construct Strategy. Here we validate the construct strategy of negative pairs. For a fair comparison, we replace the baseline of cross entropy loss with asymmetric contrast and PNE contrast. The results are summarized in Table 5. As expected, individual anchor sets (IAS) and corresponding negatives (CN) all improve the performance of baseline, but it makes more sense to combine them to construct

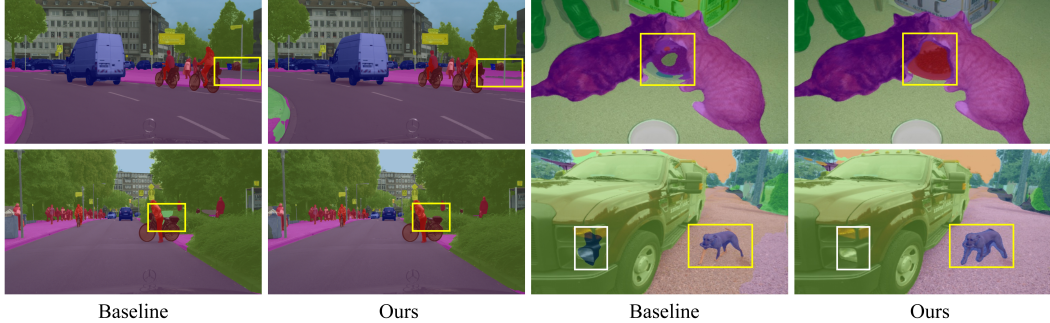


Figure 3: Visual comparison between baseline and ours (left:Cityscapes, right:COCO-Stuff).

negative pairs. Moreover, the results demonstrate that our construct strategy of negative pairs is suitable for PNE contrast.

Table 4: Ablation study for effectiveness of contrast. D-ResNet denotes the dilated-ResNet with the output stride= 8

Pixel Contrast	Backbone	mIoU%
Base (w/o Contrast)	D-ResNet-50	76.4
Base (w/o Contrast)	D-ResNet-101	78.5
Asymmetric Contrast (Eq.1)	D-ResNet-50	77.5(+1.1)
Asymmetric Contrast (Eq.1)	D-ResNet-101	79.1(+0.6)
PNE Contrast	D-ResNet-50	80.3(+3.9)
PNE Contrast	D-ResNet-101	80.8(+2.3)

Table 6: Ablation study for Per-positive weights. PW Represents Per-positive weights.

Per-positives weights	std	mIoU%
PNE Contrast (w/o PW)	-	80.1
PNE Contrast (PW w/o <i>softmax</i>)	1.547	80.1
PNE Contrast (PW w <i>softmax</i>)	0.112	80.3

Per-positive weights. We also implement experiments to evaluate the significance of Per-positive weights. As shown in Table 6, our method reaches better result with per-positive weights. Proving that the measure of similarity is not enough to fully utilize positive samples. Positive weights make the anchor pay more attention to the features with better separability. Similar to poor students learning directly from top students to get higher grades. Furthermore, the prediction scores show more stable weights after *softmax*.

Influence of hyper-parameters τ and α . we carry out experiments to assess the influence of hyper-parameters (temperature τ and PNE contrastive loss weight α). 1) Temperature τ has been investigated thoroughly and it is a consensus that τ controls the attention from loss to hard example and affects performance easily. However, in Table 7, it shows that our loss is not sensitive to temperature τ . We analysis that PNE contrast has filtered hard positive and negative pairs before calculating with temperature τ . 2) It can be clearly seen that $\alpha = 1.3$ is the sweet spot for the current baseline (D-ResNet-50). The increment or reduction of α will lead to performance deterioration.

5 Discussion and Conclusion

In this paper, we propose a novel contrastive loss for fully-supervised semantic segmentation, named Positive-Negative Equal contrastive loss, to introduce preferable distribution to hard pixels. We redesign NCE loss function by increasing the importance of positive samples to cast off the stereotype of unsupervised learning. Then, we reconstruct the negative sample pair and replace the confused

embedding similarity with explicit label information to find difficult negative samples. Our method achieves promising results on various benchmark for semantic segmentation task.

Limitation and Potential Negative Societal Impact. There are still some unsolved limitations in this paper, such as optimizing the computational efficiency of unstructured loss and more efficient sampling methods, which will be studied in future work. This work does not have the direct negative societal impact.

References

- [1] Jonathan Long, Evan Shelhamer, and Trevor Darrell. Fully convolutional networks for semantic segmentation. In *Proceedings of the IEEE conference on computer vision and pattern recognition*, pages 3431–3440, 2015.
- [2] Jun Fu, Jing Liu, Haijie Tian, Yong Li, Yongjun Bao, Zhiwei Fang, and Hanqing Lu. Dual attention network for scene segmentation. In *Proceedings of the IEEE/CVF Conference on Computer Vision and Pattern Recognition*, pages 3146–3154, 2019.
- [3] Xiaolong Wang, Ross Girshick, Abhinav Gupta, and Kaiming He. Non-local neural networks. In *Proceedings of the IEEE conference on computer vision and pattern recognition*, pages 7794–7803, 2018.
- [4] L. C. Chen, G. Papandreou, I. Kokkinos, K. Murphy, and A. L. Yuille. Deeplab: Semantic image segmentation with deep convolutional nets, atrous convolution, and fully connected crfs. *IEEE Transactions on Pattern Analysis and Machine Intelligence*, 40(4):834–848, 2018.
- [5] Fisher Yu and Vladlen Koltun. Multi-scale context aggregation by dilated convolutions. *arXiv preprint arXiv:1511.07122*, 2015.
- [6] Kaiming He, Xiangyu Zhang, Shaoqing Ren, and Jian Sun. Spatial pyramid pooling in deep convolutional networks for visual recognition. *IEEE transactions on pattern analysis and machine intelligence*, 37(9):1904–1916, 2015.
- [7] Tsung-Wei Ke, Jyh-Jing Hwang, Ziwei Liu, and Stella X Yu. Adaptive affinity fields for semantic segmentation. In *Proceedings of the European conference on computer vision (ECCV)*, pages 587–602, 2018.
- [8] Shuai Zhao, Yang Wang, Zheng Yang, and Deng Cai. Region mutual information loss for semantic segmentation. *Advances in Neural Information Processing Systems*, 32, 2019.
- [9] Ting Chen, Simon Kornblith, Mohammad Norouzi, and Geoffrey Hinton. A simple framework for contrastive learning of visual representations. In *International conference on machine learning*, pages 1597–1607. PMLR, 2020.
- [10] Kaiming He, Haoqi Fan, Yuxin Wu, Saining Xie, and Ross Girshick. Momentum contrast for unsupervised visual representation learning. In *Proceedings of the IEEE/CVF Conference on Computer Vision and Pattern Recognition*, pages 9729–9738, 2020.
- [11] Wenguan Wang, Tianfei Zhou, Fisher Yu, Jifeng Dai, Ender Konukoglu, and Luc Van Gool. Exploring cross-image pixel contrast for semantic segmentation. *arXiv preprint arXiv:2101.11939*, 2021.
- [12] Hanzhe Hu, Jinshi Cui, and Liwei Wang. Region-aware contrastive learning for semantic segmentation. In *Proceedings of the IEEE/CVF International Conference on Computer Vision*, pages 16291–16301, 2021.
- [13] Feng Wang and Huaping Liu. Understanding the behaviour of contrastive loss. In *Proceedings of the IEEE/CVF Conference on Computer Vision and Pattern Recognition*, pages 2495–2504, 2021.
- [14] Liang-Chieh Chen, George Papandreou, Florian Schroff, and Hartwig Adam. Rethinking atrous convolution for semantic image segmentation. *arXiv preprint arXiv:1706.05587*, 2017.
- [15] H. Zhao, J. Shi, X. Qi, X. Wang, and J. Jia. Pyramid scene parsing network. In *IEEE Computer Society*, 2016.
- [16] O. Ronneberger, P. Fischer, and T. Brox. U-net: Convolutional networks for biomedical image segmentation. *Springer International Publishing*, 2015.
- [17] V. Badrinarayanan, A. Kendall, and R. Cipolla. Segnet: A deep convolutional encoder-decoder architecture for image segmentation. *IEEE Transactions on Pattern Analysis & Machine Intelligence*, pages 1–1, 2017.
- [18] Y. Yuan, L. Huang, J. Guo, C. Zhang, X. Chen, and J. Wang. Ocnet: Object context for semantic segmentation. *International Journal of Computer Vision*, pages 1–24, 2021.
- [19] Yuhui Yuan, Xilin Chen, and Jingdong Wang. Object-contextual representations for semantic segmentation. In *Computer Vision–ECCV 2020: 16th European Conference, Glasgow, UK, August 23–28, 2020, Proceedings, Part VI 16*, pages 173–190. Springer, 2020.

[20] Sixiao Zheng, Jiachen Lu, Hengshuang Zhao, Xiatian Zhu, Zekun Luo, Yabiao Wang, Yanwei Fu, Jianfeng Feng, Tao Xiang, Philip HS Torr, et al. Rethinking semantic segmentation from a sequence-to-sequence perspective with transformers. In *Proceedings of the IEEE/CVF Conference on Computer Vision and Pattern Recognition*, pages 6881–6890, 2021.

[21] Robin Strudel, Ricardo Garcia, Ivan Laptev, and Cordelia Schmid. Segmenter: Transformer for semantic segmentation. *arXiv preprint arXiv:2105.05633*, 2021.

[22] Alexey Dosovitskiy, Lucas Beyer, Alexander Kolesnikov, Dirk Weissenborn, Xiaohua Zhai, Thomas Unterthiner, Mostafa Dehghani, Matthias Minderer, Georg Heigold, Sylvain Gelly, et al. An image is worth 16x16 words: Transformers for image recognition at scale. *arXiv preprint arXiv:2010.11929*, 2020.

[23] Aaron van den Oord, Yazhe Li, and Oriol Vinyals. Representation learning with contrastive predictive coding. *arXiv preprint arXiv:1807.03748*, 2018.

[24] Zhirong Wu, Yuanjun Xiong, Stella X Yu, and Dahua Lin. Unsupervised feature learning via non-parametric instance discrimination. In *Proceedings of the IEEE conference on computer vision and pattern recognition*, pages 3733–3742, 2018.

[25] Ting Chen, Simon Kornblith, Kevin Swersky, Mohammad Norouzi, and Geoffrey Hinton. Big self-supervised models are strong semi-supervised learners. *arXiv preprint arXiv:2006.10029*, 2020.

[26] Ishan Misra and Laurens van der Maaten. Self-supervised learning of pretext-invariant representations. In *Proceedings of the IEEE/CVF Conference on Computer Vision and Pattern Recognition*, pages 6707–6717, 2020.

[27] Xinlei Chen, Haoqi Fan, Ross Girshick, and Kaiming He. Improved baselines with momentum contrastive learning. *arXiv preprint arXiv:2003.04297*, 2020.

[28] Yannis Kalantidis, Mert Bulent Sariyildiz, Noe Pion, Philippe Weinzaepfel, and Diane Larlus. Hard negative mixing for contrastive learning. *arXiv preprint arXiv:2010.01028*, 2020.

[29] Prannay Khosla, Piotr Teterwak, Chen Wang, Aaron Sarna, Yonglong Tian, Phillip Isola, Aaron Maschinot, Ce Liu, and Dilip Krishnan. Supervised contrastive learning. *arXiv preprint arXiv:2004.11362*, 2020.

[30] Joshua Robinson, Ching-Yao Chuang, Suvrit Sra, and Stefanie Jegelka. Contrastive learning with hard negative samples. *arXiv preprint arXiv:2010.04592*, 2020.

[31] K. Chaitanya, E. Erdil, N. Karani, and E. Konukoglu. Contrastive learning of global and local features for medical image segmentation with limited annotations. 2020.

[32] Xinlong Wang, Rufeng Zhang, Chunhua Shen, Tao Kong, and Lei Li. Dense contrastive learning for self-supervised visual pre-training, 2021.

[33] Z. Xie, Y. Lin, Z. Zhang, Y. Cao, and H. Hu. Propagate yourself: Exploring pixel-level consistency for unsupervised visual representation learning. 2020.

[34] Zhenchao Jin, Tao Gong, Dongdong Yu, Qi Chu, Jian Wang, Changhu Wang, and Jie Shao. Mining contextual information beyond image for semantic segmentation. In *Proceedings of the IEEE/CVF International Conference on Computer Vision*, pages 7231–7241, 2021.

[35] Christian Szegedy, Vincent Vanhoucke, Sergey Ioffe, Jon Shlens, and Zbigniew Wojna. Rethinking the inception architecture for computer vision. In *Proceedings of the IEEE conference on computer vision and pattern recognition*, pages 2818–2826, 2016.

[36] Geoffrey Hinton, Oriol Vinyals, Jeff Dean, et al. Distilling the knowledge in a neural network. *arXiv preprint arXiv:1503.02531*, 2(7), 2015.

[37] Yizhou Wang, Shixiang Tang, Feng Zhu, Lei Bai, Rui Zhao, Donglian Qi, and Wanli Ouyang. Revisiting the transferability of supervised pretraining: an mlp perspective. *arXiv preprint arXiv:2112.00496*, 2021.

[38] MM Segmentation Contributors. MM Segmentation: Openmmlab semantic segmentation toolbox and benchmark. <https://github.com/open-mmlab/mmsegmentation>, 2020.

[39] Adam Paszke, Sam Gross, Francisco Massa, Adam Lerer, James Bradbury, Gregory Chanan, Trevor Killeen, Zeming Lin, Natalia Gimelshein, Luca Antiga, et al. Pytorch: An imperative style, high-performance deep learning library. *Advances in neural information processing systems*, 32, 2019.

[40] Liang-Chieh Chen, Yukun Zhu, George Papandreou, Florian Schroff, and Hartwig Adam. Encoder-decoder with atrous separable convolution for semantic image segmentation. In *Proceedings of the European conference on computer vision (ECCV)*, pages 801–818, 2018.

[41] Hengshuang Zhao, Jianping Shi, Xiaojuan Qi, Xiaogang Wang, and Jiaya Jia. Pyramid scene parsing network. In *Proceedings of the IEEE conference on computer vision and pattern recognition*, pages 2881–2890, 2017.

[42] Sungha Choi, Joanne T Kim, and Jaegul Choo. Cars can't fly up in the sky: Improving urban-scene segmentation via height-driven attention networks. In *Proceedings of the IEEE/CVF conference on computer vision and pattern recognition*, pages 9373–9383, 2020.

- [43] Xia Li, Yibo Yang, Qijie Zhao, Tiancheng Shen, Zhouchen Lin, and Hong Liu. Spatial pyramid based graph reasoning for semantic segmentation. In *Proceedings of the IEEE/CVF Conference on Computer Vision and Pattern Recognition*, pages 8950–8959, 2020.
- [44] Fan Zhang, Yanqin Chen, Zhihang Li, Zhibin Hong, Jingtuo Liu, Feifei Ma, Junyu Han, and Errui Ding. Acfnet: Attentional class feature network for semantic segmentation. In *Proceedings of the IEEE/CVF International Conference on Computer Vision*, pages 6798–6807, 2019.
- [45] Hang Zhang, Kristin Dana, Jianping Shi, Zhongyue Zhang, Xiaogang Wang, Ambrish Tyagi, and Amit Agrawal. Context encoding for semantic segmentation. In *Proceedings of the IEEE conference on Computer Vision and Pattern Recognition*, pages 7151–7160, 2018.
- [46] Henghui Ding, Xudong Jiang, Bing Shuai, Ai Qun Liu, and Gang Wang. Semantic correlation promoted shape-variant context for segmentation. In *Proceedings of the IEEE/CVF Conference on Computer Vision and Pattern Recognition*, pages 8885–8894, 2019.
- [47] Jun Fu, Jing Liu, Yuhang Wang, Yong Li, Yongjun Bao, Jinhui Tang, and Hanqing Lu. Adaptive context network for scene parsing. In *Proceedings of the IEEE/CVF International Conference on Computer Vision*, pages 6748–6757, 2019.
- [48] Tete Xiao, Yingcheng Liu, Bolei Zhou, Yuning Jiang, and Jian Sun. Unified perceptual parsing for scene understanding. In *Proceedings of the European Conference on Computer Vision (ECCV)*, pages 418–434, 2018.
- [49] Ze Liu, Yutong Lin, Yue Cao, Han Hu, Yixuan Wei, Zheng Zhang, Stephen Lin, and Baining Guo. Swin transformer: Hierarchical vision transformer using shifted windows. In *Proceedings of the IEEE/CVF International Conference on Computer Vision*, pages 10012–10022, 2021.
- [50] Hang Zhang, Han Zhang, Chenguang Wang, and Junyuan Xie. Co-occurrent features in semantic segmentation. In *Proceedings of the IEEE/CVF Conference on Computer Vision and Pattern Recognition*, pages 548–557, 2019.
- [51] Zilong Huang, Xinggang Wang, Lichao Huang, Chang Huang, Yunchao Wei, and Wenyu Liu. Ccnet: Criss-cross attention for semantic segmentation. In *Proceedings of the IEEE/CVF International Conference on Computer Vision*, pages 603–612, 2019.
- [52] Pingping Zhang, Wei Liu, Hongyu Wang, Yinjie Lei, and Huchuan Lu. Deep gated attention networks for large-scale street-level scene segmentation. *Pattern Recognition*, 88:702–714, 2019.

A Appendix

A.1 Visual comparison of pixel embeddings by t-SNE

To prove the validity of PNE loss proposed, we visualize the distribution of pixel embeddings, as shown in Fig.4. The uniformity(inter-class) and alignment(intra-class) of pixel embeddings are obtained substantial advance after plugging the PNE loss. For uniformity, \bullet (vegetation) and \bullet (building) are separated more clearly with our method. For alignment, \bullet (pole) are divided into three parts in different context, but aggregated unitedly as a whole in the Fig.(b) with more closeness. That greatly demonstrates PNE loss can assist model to capture the relationships between pixels and improve segmentation accuracy.

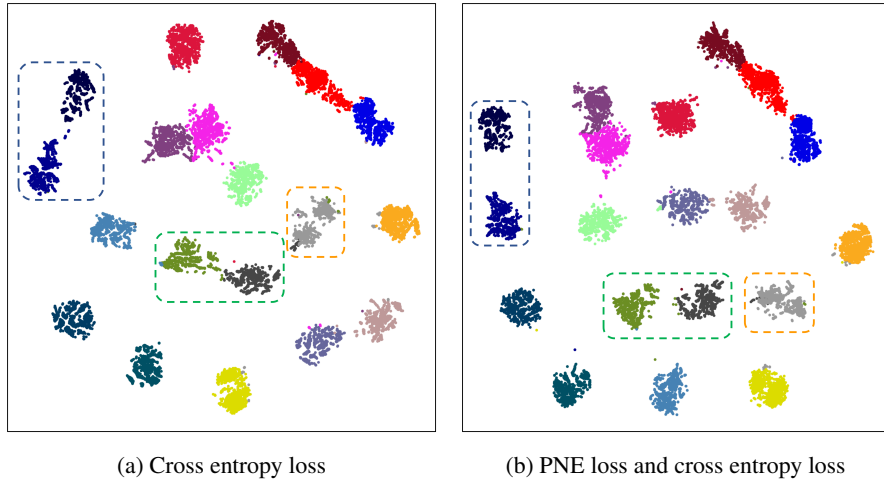


Figure 4: Visual comparison of the distribution of pixel embeddings by t-SNE. Each point represents the feature representation of a pixel. The similarity of pixel are exhibited by the distance between each point.

A.2 More visual comparison of semantic segmentation



Figure 5: More visual comparison of segmentation results on COCO-Stuff.